Science Advances
AAAS

advances.sciencemag.org/cgi/content/full/5/5/eaaw1507/DC1

Supplementary Materials for

Food antigens drive spontaneous IgE elevation in the absence of commensal microbiota

Sung-Wook Hong*, Eunju O, Jun Young Lee, Minji Lee, Daehee Han, Hyun-Ja Ko, Jonathan Sprent, Charles D. Surh, Kwang Soon Kim*

*Corresponding author. Email: kskim27@postech.ac.kr (K.S.K.); rozhzor@gmail.com (S.-W.H.)

Published 22 May 2019, *Sci. Adv.* **5**, eaaw1507 (2019)
DOI: 10.1126/sciadv.aaw1507

This PDF file includes:

Supplementary Materials

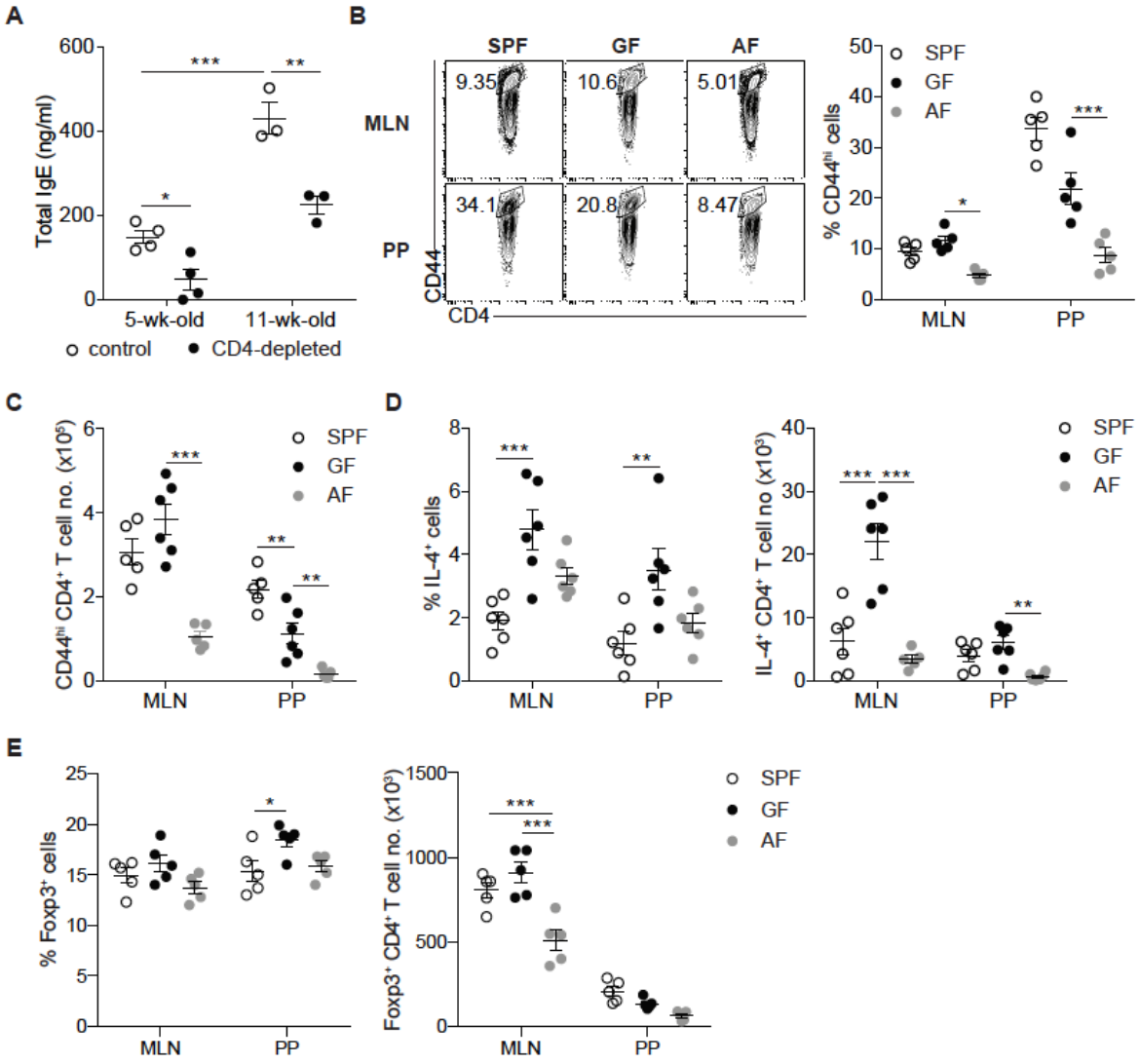

Fig. S1. MLN and PP of GF mice are major sites for T_H2-skewed immune response against food Ags. (**A**) Serum IgE levels in 5-wk or 11-wk-old GF mice after treatment with anti-CD4 depleting antibody (120 μg/mouse) twice a week for 3 wks (n=4 for 5-wk-old mice, n=3 for 11-wk-old mice). (**B**) Representative FACS plot of CD44 and CD4 (left) and the frequency of $CD44^{hi}$ activated $CD4^+$ T cells (right) gated on live $CD4^+$ $TCR\beta^+$ $Foxp3^-$ cells in MLN and PP from 10-wk-old GF and AF mice (n=5). (**C**) The number of $CD44^{hi}$ activated $CD4^+$ T cells at indicated tissues. (**D**) The frequency of IL-4-producing cells gated on $CD4^+$

TCRβ^{+} CD44^{hi} cells (left) and the number of IL-4-producing CD4^{+} T cells (right) in MLN and PP from 10-wk-old SPF, GF and AF mice (n=6). (**E**) The frequency of Foxp3^{+} cells gated on CD4^{+} TCRβ^{+} cells (left) and the number of Foxp3^{+} CD4^{+} T cells (right) in MLN and PP from 10-wk-old SPF, GF and AF mice (n=5). Data in (A) are representative of two independent experiments and data in (B-E) are pooled from two or three independent experiments. Each symbol represents an individual mouse. *P*-value was determined by two-way or one-way ANOVA with Tukey's multiple comparisons test. **P*<0.05, ***P*<0.01, ****P*<0.001. Error bars indicate SEM.

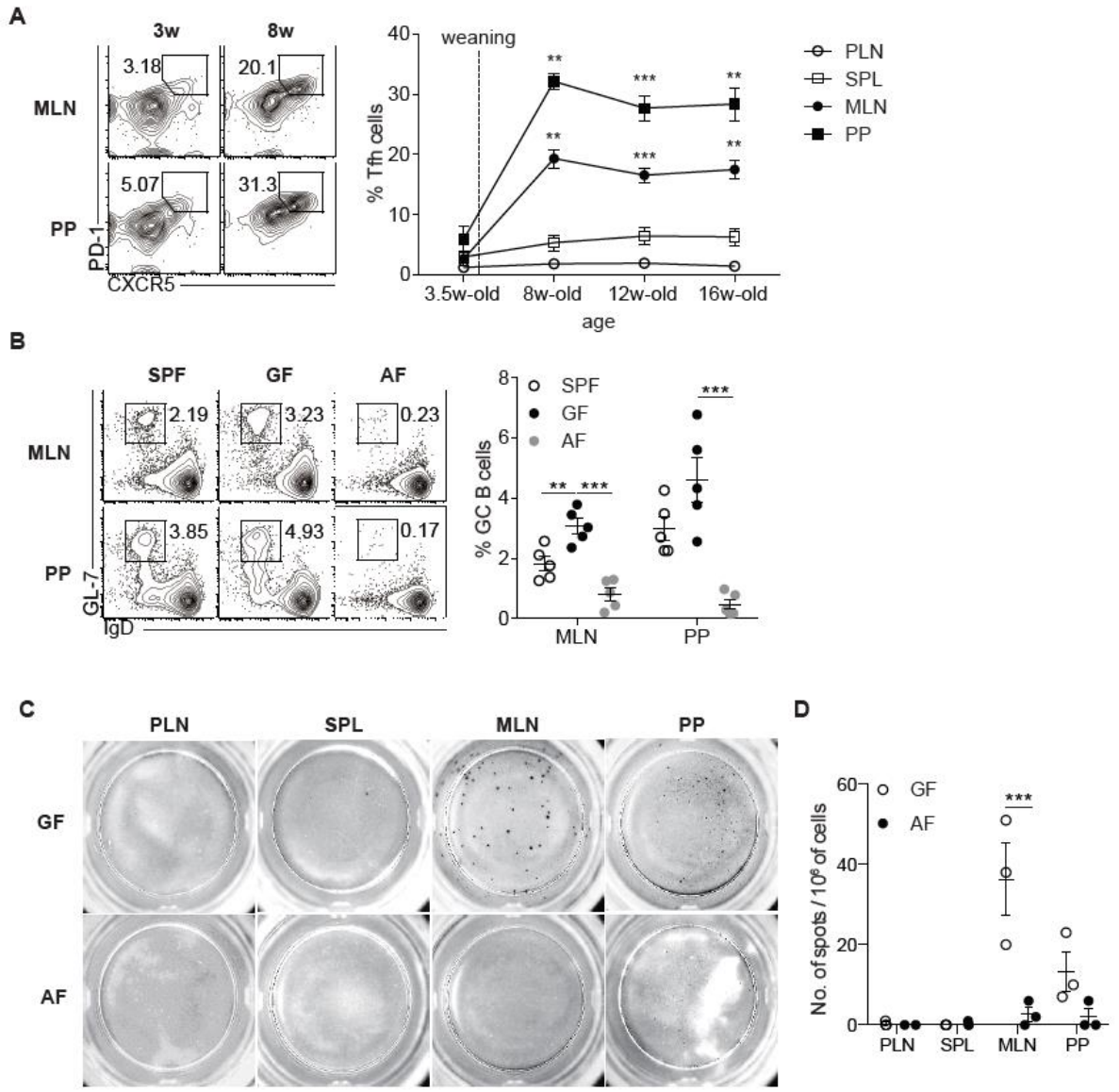

Fig. S2. T_{FH} cells in MLN and PP of GF mice are generated upon weaning onto NCD, and AF mice displayed impaired generation of GC B cells and IgE-producing cells. (**A**) The frequency of PD-1^{hi} $CXCR5^{+}$ T_{FH} cells gated on $CD4^{+}$ $TCR\beta^{+}$ $Foxp3^{-}$ $CD44^{hi}$ cells in PLN, SPL, MLN and PP from GF mice at indicated ages (n=3 per each time point). Dashed line indicates time point for weaning. (**B**) Representative FACS plot of GL-7 and IgD (left) and the frequency of GL-7^{hi} IgD^{lo} GC B cells (right) gated on $B220^{+}$ cells (n=5). (**C**) Representative ELISPOT wells for IgE-producing cells in indicated tissues. (**D**) The number

of IgE-producing cells in indicated tissues (n=3). Data in (B, D) are representative of three independent experiments. Each symbol represents an individual mouse. *P*-value was determined by one-way ANOVA with Tukey's multiple comparisons test. $^{**}P<0.01$, $^{***}P<0.001$. Error bars indicate SEM.

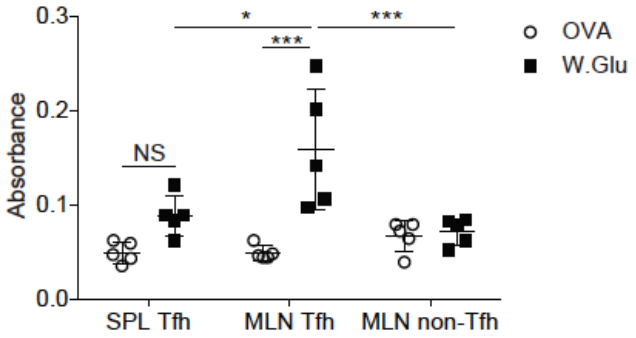

Fig. S3. Levels of wheat gluten–specific IgE in GF *Rag1*$^{-/-}$ mice cotransferred with naïve B cells and indicated CD4^{+} T cell subsets. As described in Figure 2G, FACS-sorted T_{FH} cells and non-T_{FH} cells in MLN, and T_{FH} cells in SPL from 9-12-wk-old GF mice were co-transferred into GF *Rag1*$^{-/-}$ mice with naïve B cells isolated from SPF mice. Sera were harvested at 2 wks after transfer, levels of IgE specific to wheat gluten were measured (n=5). Data are pooled from two independent experiments. Each symbol represents an individual mouse. *P*-value was determined by two-way ANOVA with Tukey's multiple comparisons test. **P*<0.05, ****P*<0.001. NS, not significant. Error bars indicate SEM.

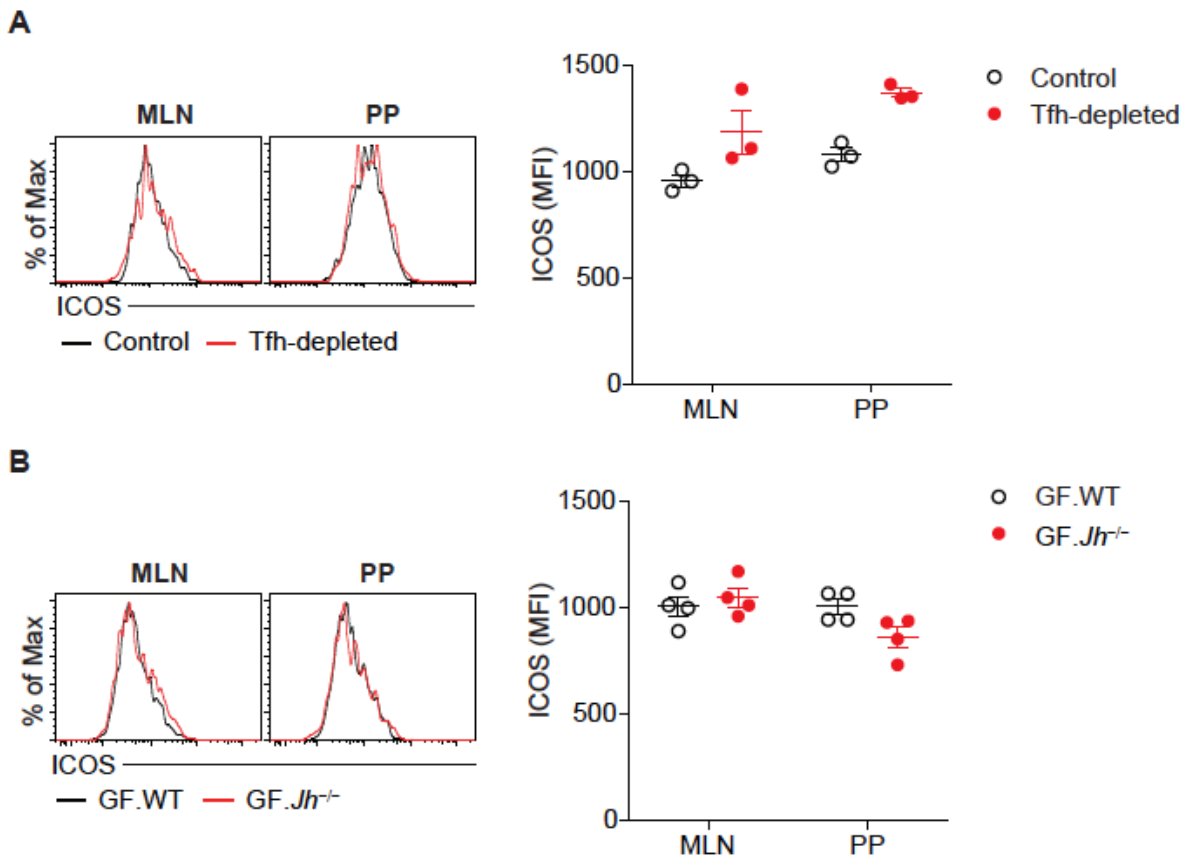

Fig. S4. ICOS up-regulation on activated CD4$^+$ T cells is independent on the presence of T_{FH} cells and B cells. (**A**) Representative histograms (left) and MFI of ICOS expression (right) on CD44^{hi} activated CD4$^+$ T cells (live CD4$^+$ TCRβ$^+$ Foxp3$^-$ CD44^{hi}) in MLN and PP from untreated GF mice (control) and GF mice treated with anti-ICOSL antibody (T_{FH}-depleted) (n=3). (**B**) Representative histograms (left) and MFI of ICOS expression (right) on CD44^{hi} activated CD4$^+$ T cells cells in MLN and PP from GF WT and *Jh*$^{-/-}$ mice (n=4). Data are representative of two or three independent experiments. Each symbol represents an individual mouse. Error bars indicate SEM.

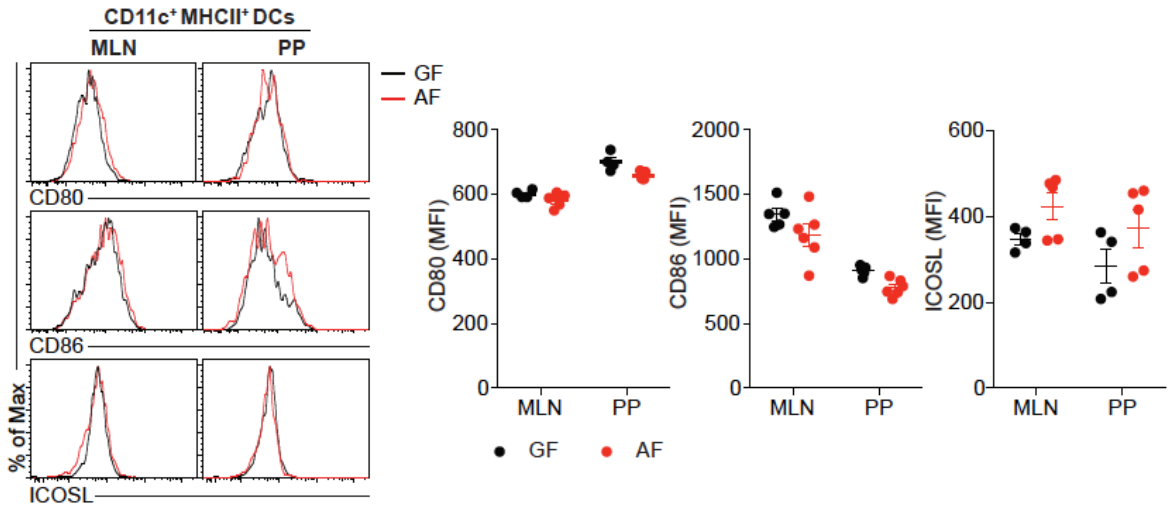

Fig. S5. Expression levels of CD80, CD86, and ICOSL on MLN and PP DCs are comparable between GF and AF mice. Representative histograms (left) and MFI (right) of CD80, CD86 and ICOSL on live CD11c^{+} MHCII^{+} B220^{-} DCs in MLN and PP from 9-wk-old GF and AF mice (n=4~6). Data are pooled from two independent experiments. Each symbol represents an individual mouse. Error bars indicate SEM.

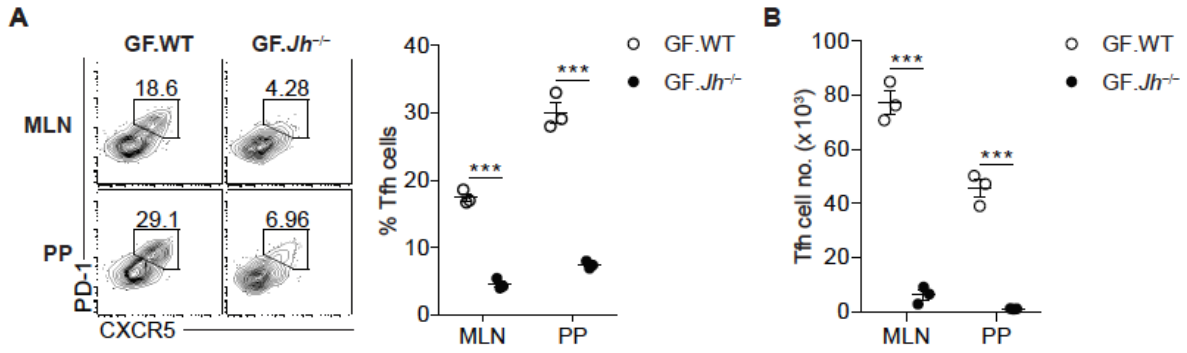

Fig. S6. B cells are required for the generation of food Ag–driven T_{FH} cells in GALT. (**A**) Representative FACS plot of CXCR5 and PD-1 (left) and the frequency of PD-1^{hi} $CXCR5^{+}$ T_{FH} cells (right) gated on $CD4^{+}$ $TCR\beta^{+}$ $Foxp3^{-}$ $CD44^{hi}$ cells in MLN and PP of 9~10-wk-old GF WT and *Jh*$^{-/-}$ mice (n=3). (**B**) The number of T_{FH} cells in indicated tissues from GF WT and *Jh*$^{-/-}$ mice. Data are representative of three independent experiments. Each symbol represents an individual mouse. Statistical differences were determined by two-way ANOVA with Tukey's multiple comparisons test. ***P<0.001. Error bars indicate SEM.

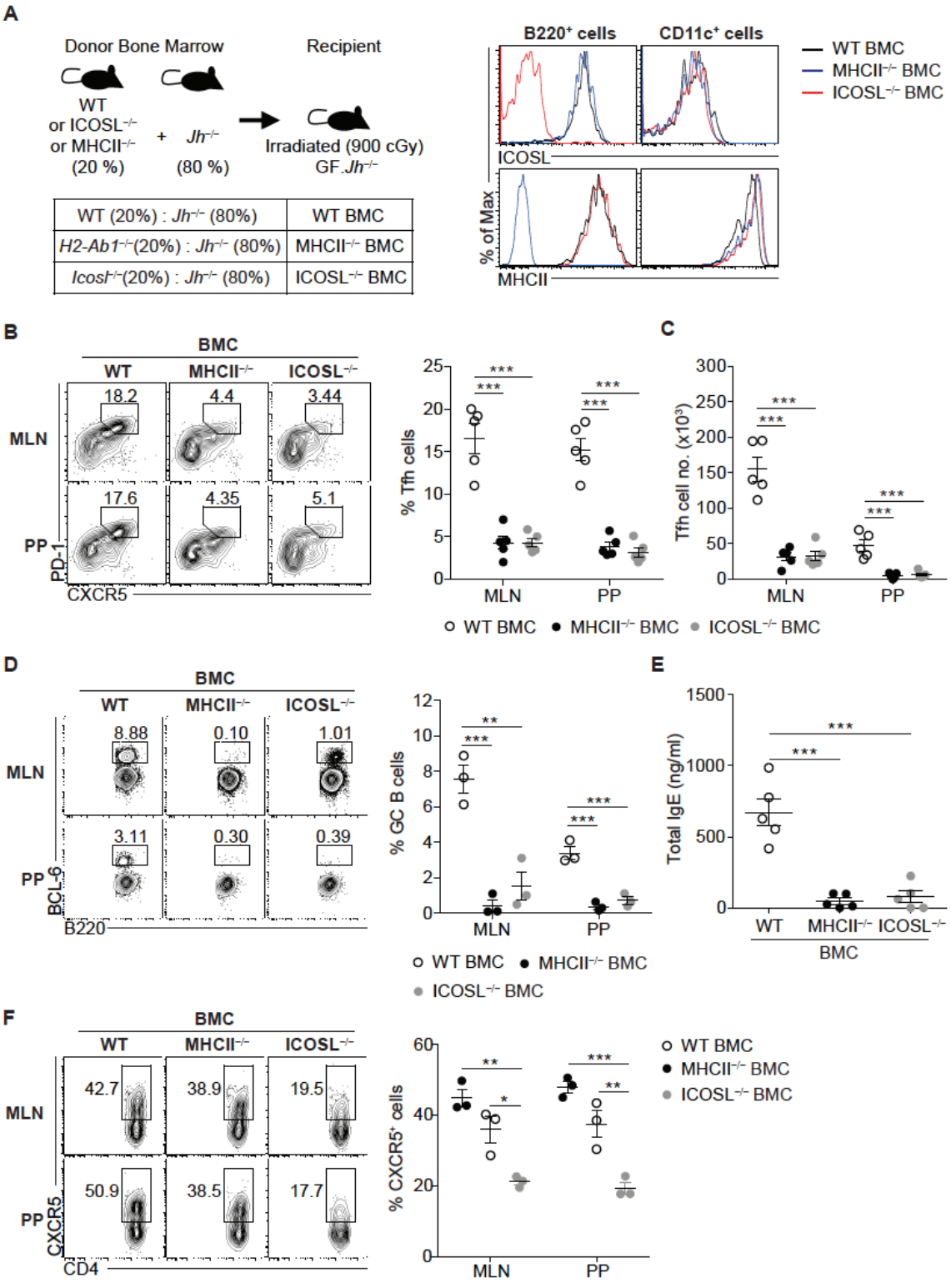

Fig. S7. B cells promote terminal differentiation of food Ag–driven TFH cells by providing ICOS signaling and presenting cognate Ags. Mixed bone marrow chimeras (BMCs) were generated by reconstituting lethally irradiated (900 cGy) GF *Jh*$^{-/-}$ mice with

8:2 mixture of *Jh*$^{-/-}$ BM cells and either *Icosl*$^{-/-}$ (ICOSL$^{-/-}$ BMC) or *H2-Ab1*$^{-/-}$ (MHCII$^{-/-}$ BMC) BM cells. As a control, BMCs with a mixture of *Jh*$^{-/-}$ and WT BM cells were used. BMCs were analyzed at 6 wks after BM reconstitution. (**A**) Schematic view of mixed BMC generation (left) and representative histograms showing ICOSL (top) and MHCII (bottom) expression levels on B220^{+} cells and CD11c^{+} cells in indicated mixed BMC. (**B**) Representative FACS plots of CXCR5 and PD-1 (left) and the frequency of PD-1^{hi} CXCR5^{+} T_{FH} cells (right) gated on live CD4^{+} TCRβ^{+} Foxp3^{-} CD44^{hi} cells in MLN and PP of indicated BMCs. (**C**) Number of PD-1^{hi} CXCR5^{+} T_{FH} cells in MLN and PP of indicated BMCs. (**D**) Representative FACS plot of BCL-6 and B220 (left) and the frequency of B220^{+} BCL-6^{+} GC B cells (right) gated on live B220^{+} cells (n=3). (**E**) Serum IgE levels of indicated BMCs (n=5). (**F**) Representative FACS plot of CXCR5 and CD4 (left) and the frequency of CXCR5-expressing cells (right) gated on live CD4^{+} TCRβ^{+} Foxp3^{-} CD44^{hi} cells (n=3). Data in (A, D, F) are representative of two independent experiments. Data from two independent experiments are pooled (B, C, E). Each symbol represents an individual mouse. *P*-value was determined by one-way ANOVA with Tukey's multiple comparisons test. **P*<0.05, ***P*<0.01, ****P*<0.001. Error bars indicate SEM.

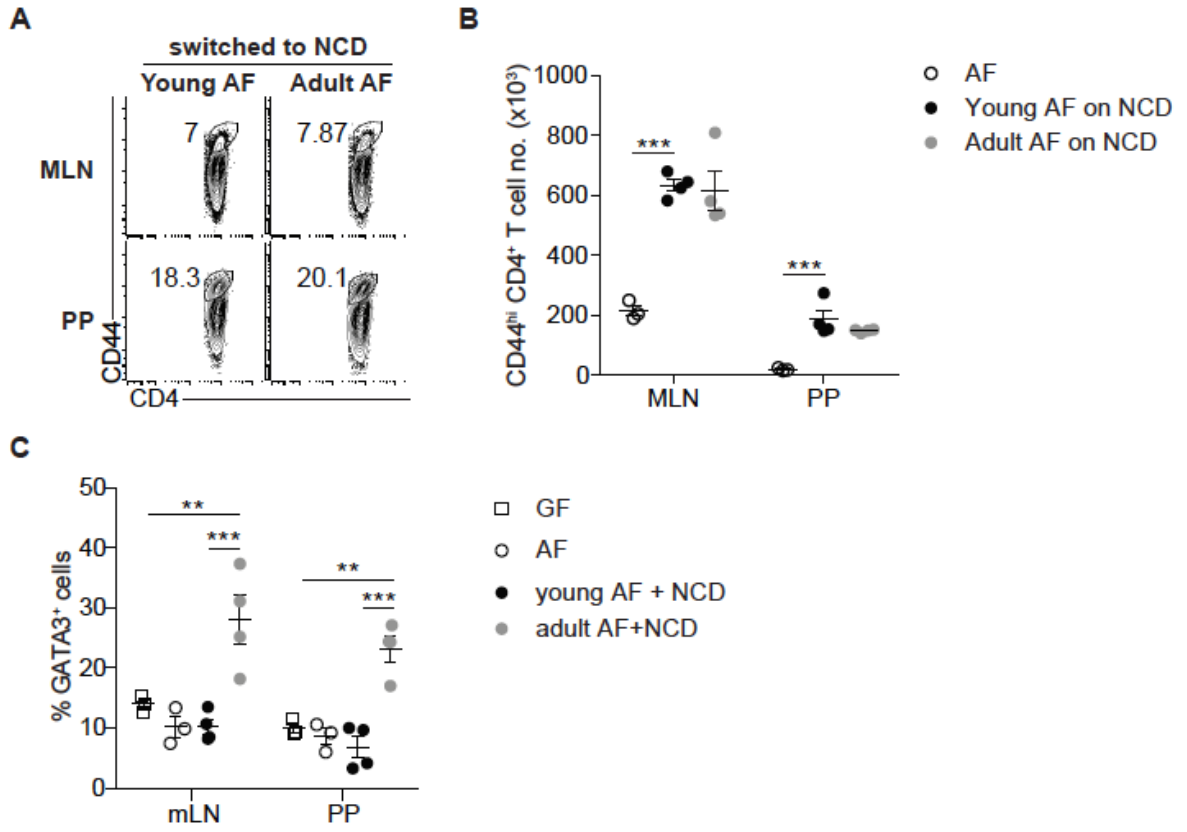

Fig. S8. Levels of CD4$^+$ T cell activation in MLN and PP are comparable between young and adult AF mice switched to NCD, but the latter shows increased levels of T$_H$2 cells. Young and adult AF mice (4 wks old and 8 wks old, respectively) were switched to NCD for 4 wks. (**A** and **B**) Representative FACS plot of CD44 and CD4 (A) and the number of CD44^{hi} CD4$^+$ T cells (B) gated on live CD4$^+$ TCRβ$^+$ Foxp3$^-$ cells in MLN and PP (n=3~4). (**C**) The frequency of GATA3$^+$ cells gated on live CD44^{hi} CD4$^+$ TCRβ$^+$ Foxp3$^-$ cells in MLN and PP in indicated mice (n=3~4). Data are representative of two independent experiments. Each symbol represents an individual mouse. *P*-value was determined by one-way ANOVA with Tukey's multiple comparisons test. ***P*<0.01, ****P*<0.001. Error bars indicate SEM.

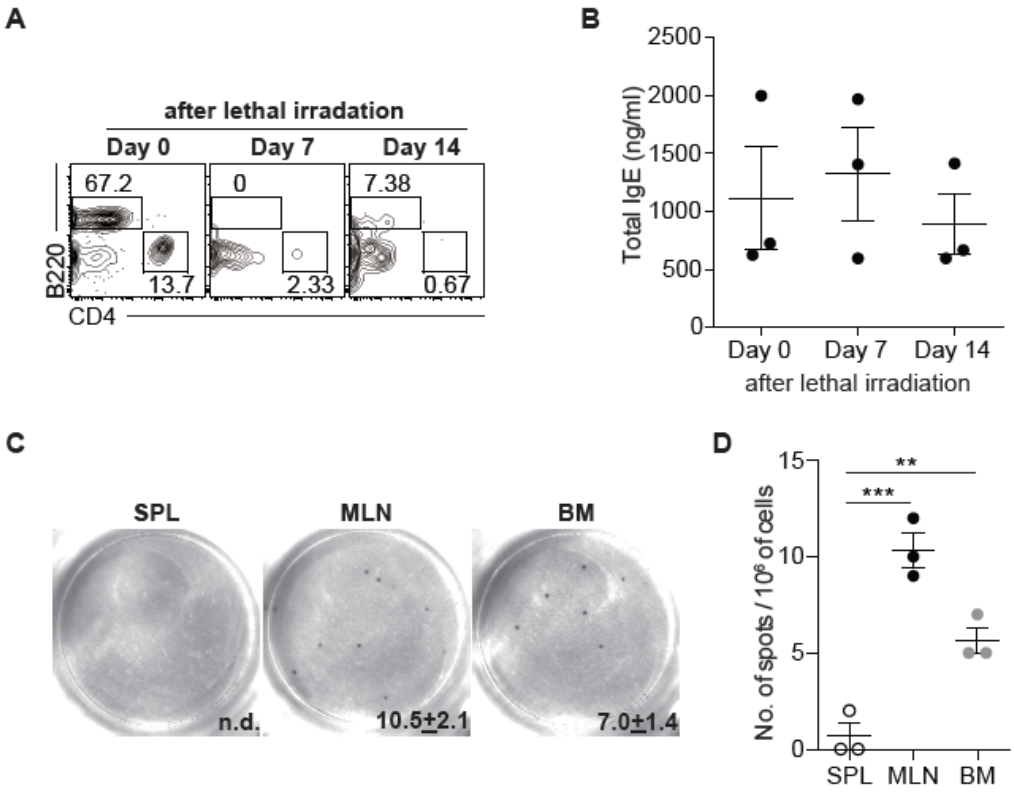

Fig. S9. High serum IgE levels in adult GF mice are sustained by radioresistant long-lived IgE-producing cells in MLN and BM. 14-wk-old GF mice were lethally irradiated (900 cGy) and reconstituted with *Rag1*$^{-/-}$ BM cells. (**A**) Representative FACS plot showing the depletion of CD4^{+} T cells and B cells in blood (n=3). (**B**) Serum IgE levels at day 0, 7 and 14 after irradiation were measured by ELISA. (**C**) IgE-producing cells at indicated tissues were examined by ELISPOT at 2 wks after irradiation. (**D**) The number of IgE-producing cells at indicated tissues (n=3). *P*-value was determined by one-way ANOVA with Tukey's multiple comparisons test. ***P*<0.05, ****P*<0.001. Error bars indicate SEM.

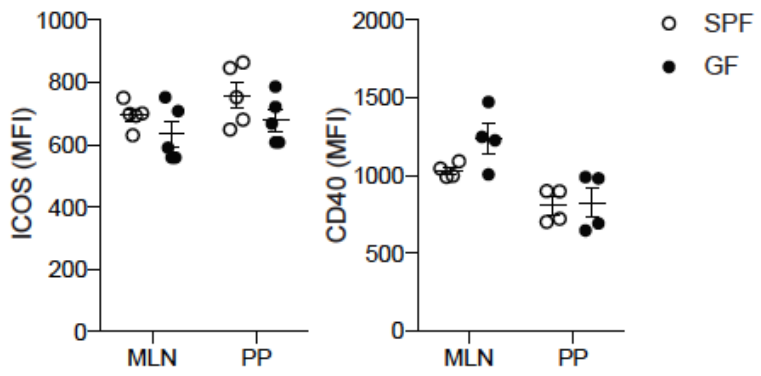

Fig. S10. ICOS expression on activated CD4$^+$ T cells and CD40 expression on DCs in MLN and PP in SPF mice are both comparable with those in GF mice. Single cell suspension was prepared from MLN and PP of 9~10-wk-old GF and SPF mice to examine ICOS and CD40 expression on activated CD4$^+$ T cells and DCs, respectively (n=4~5). MFI of ICOS expression on CD44^{hi} CD4 T cells (left) and MFI of CD40 expression on CD11c$^+$ MHCII$^+$ DCs (right) were shown. Data are representative of two independent experiments (n=4~5). Each symbol represents an individual mouse. Error bars indicate SEM.